Experiment and Model for Distance-Dependent Mismatch

Ning Lu*, Noah Zamdmer**, and Richard Wachnik**
*IBM Systems, Essex Junction, VT 05452 USA lun@us.ibm.com
**IBM Systems, Hopewell Junction, NY 12533 USA

ABSTRACT

Model of across-chip variation that is accurate for both the micrometer and the millimeter scale enables chip designers to improve power, performance, and yield. Through theory and experimental data, we first show that distance-dependent mismatch in semiconductor devices exhibits a relation that deviates from Pelgrom's quadratic-in- distance relation, especially for large distance. Next, for the first time, we present a compact and complete solution of modeling any arbitrarily given 1D or 2D distance-dependent mismatch and spatial correlations. The resulting spatial correlation is both translational invariant and continuous. The correlation range of the given spatial correlation can be much smaller than, be about, or be much larger than chip size. When netlisting each device for simulations, we only need that device's location.

Keywords: statistical model, distance-dependent mismatch, across-chip variations, modeling of spatial correlations

1. INTRODUCTION

The difference in electric characteristics between identically designed devices/logic gates (called mismatch typically) is a very real concern for circuit designers. Over the past 30 years, semiconductor device and modeling engineers have investigated, characterized, and modeled adjacent mismatch extensively [1, 2, 3]. The mismatch in device and/or circuit level arises from mismatch in various semiconductor process steps. Best design practices have been adopted to reduce device/circuit mismatch. Mismatch among multiple devices separated by finite distances has received limited attention [1, 2, 4]. This mismatch can be both systematic by location [4] and random [1]. As systematic mismatch can often be suppressed, this paper focuses on the less-avoidable random component. One well-known distance-dependent mismatch relation is Pelgrom's quadratic relationship with device separation [1]. In the electronic design automation (EDA) community, the problem of modeling spatial correlation has been extensively studied over the past 15 years. All those studies, however, either use a grid or block representation [5], resulting a not-always-continuous solution and thus not being suitable for mismatch modeling, or use the eigen vector method to solve an NxN correlation matrix for a group of N separated devices, resulting a lengthy solution plus requiring knowing device number N and all device locations in advance. None of solutions presented in the EDA community is suitable for being implemented in a SPICE model by a foundry company and later delivered to its fabless customers.

In this paper, we study (i) distance-dependent mismatch and (ii) spatial correlation problems both experimentally and theoretically. The two problems are intimately connected. We present our hardware results and, using the relationship between mismatch and correlation, show that the relationship between mismatch and distance must deviate from the well-known Pelgrom quadratic relationship when the distance is large. For the first time, we present a compact and complete solution of modeling both distance-dependent mismatch and spatial correlation problems. We show how to model an arbitrarily given shape of mismatch or correlation vs. distance relation. Explicit analytic solution for modeling each of Gaussian, exponential, Lorentz, and linear decreasing types of spatial correlation is given. There are no grid points, no brackets, and no matrix solution in our method. Both model-generated spatial correlation and mismatch are translational invariant and continuous. The correlation range of spatial correlation can be much smaller than chip size, be about the chip size, or be much larger than chip size. Our method produces a very compact Monte Carlo model for SPICE or TCAD simulation, and it enables a simultaneous modeling of $N(N-1)/2$ pairs of mismatch relations among N devices/circuits, regardless of the physical locations of the N devices/circuits. Our method is very compact, since we do not use a matrix or a set of eigen solutions to represent correlations among a group of devices/circuits.

2. CHARACTERIZATIONS OF ACROSS-CHIP VARIATIONS

To measure and characterize across-chip variations (ACV), dozens ring oscillators or FETs were placed on SOI technology [6, 7] chips. The delay of ROs at various chip locations was measured on many wafers. The delay mismatch between each pair of ROs was calculated, and then was plotted vs. their separation (Fig. 1). A best-fit mismatch vs. distance relation was determined. ACV can also be analyzed in terms of correlation coefficient vs. distance, since mismatch and correlation coefficient for a parameter P are related,

$$\left\langle [P_i(\mathbf{x}_i) - P_j(\mathbf{x}_j)]^2 \right\rangle / 2\sigma^2 + C(\mathbf{x}_i, \mathbf{x}_j) = 1. \qquad (1)$$

Using the notation of [8], P_i is the ith device's parameter, $\mathbf{x}_i = (x_i, y_i)$ is the location of the ith device, and

$$\sigma^2 \equiv \left\langle [P_i(\mathbf{x}_i) - \langle P_i(\mathbf{x}_i) \rangle]^2 \right\rangle = \sigma_{sys}^2 + \sigma_{acv}^2 + \tfrac{1}{2}\sigma_{m0}^2 \qquad (2)$$

is the total variance of $P_i(\mathbf{x}_i)$ with i = 1, 2, 3, …. Also, (i) σ_{sys}^2, (ii) σ_{acv}^2, and (iii) $\frac{1}{2}\sigma_{m0}^2$ are (i) completely correlated, (ii) distance-dependent and partially correlated, and (iii) completely uncorrelated parts of total variance, respectively (Fig. 2). Correlation coefficient is a normalized variable, whereas mismatch itself is not. The first term in (1) is a normalized mismatch. Figures 3 and 4 show how a correlation coefficient vs. distance relation was obtained. Extrapolating

the distance-dependent curve toward zero distance, the resulting correlation coefficient is smaller than unity. This can be understood in terms of the existence of adjacent mismatch (σ_{m0}). Besides measuring and analyzing RO delay, FET drain current and threshold voltages at multiple locations of each chip were also measured and plotted to characterize distance-dependent correlation coefficient and/or mismatch. Figures 5 and 6 show scatter plots of mismatch and correlation coefficient of FinFET's linear threshold voltage vs. distance for 14nm SOI FinFET technology [7], along with characterized distance-dependent relations. Pelgrom's characterization on distance-dependent mismatch is [1]

$$\left\langle [P_i(\mathbf{x}_i) - P_j(\mathbf{x}_j)]^2 \right\rangle = \sigma_{m0}^2 + b(x_{ij}^2 + y_{ij}^2), \quad i \neq j, \qquad (3)$$

where b is a technology and device dependent parameter, $x_{ij} = x_i - x_j$, and $y_{ij} = y_i - y_j$. Since a correlation coefficient has an absolute lower bound of –1, and here a practical lower bound of zero, there is an upper bound for mismatch according to relation (1). Thus, relation (3) can be valid for a small distance, but is not valid for a large distance (say, when a distance is close to a correlation range). This conclusion is also supported by hardware data shown in Figs. 1 and 5.

3. MODELING OF ACROSS-CHIP VARIATIONS

We present a set of complete across-chip variation model in this paper. We consider a semiconductor device/circuit parameter P for a group of devices or circuits. We even do not need to know the number of devices/circuits when we build a distance-dependent variation model for them. We want to model the spatial correlations among multiple parameters P_1, P_2, P_3, P_4, …. All devices have a same mean value μ and also a same variance σ^2 for the parameter P. The spatial correlation between any two devices depends only on the coordinate differences $|x_{ij}|$ and $|y_{ij}|$ between them (i.e., is translational invariant) and is a continuous function of the coordinate differences $|x_{ij}|$ and $|y_{ij}|$. Without loss of generality, it can always be written in the form of

$$C(\mathbf{x}_i, \mathbf{x}_j) = \frac{\sigma_{sys}^2}{\sigma^2} + \frac{\sigma_{acv}^2}{\sigma^2} C_{acv}\left(\frac{|x_{ij}|}{d_x}, \frac{|y_{ij}|}{d_y}\right), \quad i \neq j. \qquad (4)$$

Length parameter d_x (d_y) represents the correlation length in the X (Y) direction. Moreover, the spatial correlation decreases monotonically with increasing device separation $|x_{ij}|$ and/or $|y_{ij}|$. The (normalized) ACV correlation function has these limiting values: $C_{acv}(0, 0) = 1$ and $C_{acv}(u, v) \to 0$ as $|u| \to \infty$ and/or $|v| \to \infty$.

3.1 One-dimensional Models

In one dimension, spatial correlation (4) is simplified to

$$c(x_i, x_j) = \frac{\sigma_{sys}^2}{\sigma^2} + \frac{\sigma_{acv}^2}{\sigma^2} c_{acv,x}\left(\frac{|x_{ij}|}{d_x}\right), \qquad i \neq j. \qquad (5)$$

with $c_{acv,x}(0) = 1$ and $c_{acv,x}(\infty) = 0$. Our compact solution for modeling given 1D spatial correlation for a parameter P is [8]:

$$P(x_i) = \mu + \sigma_{sys} G_0 + \sigma_{acv}\left(G_1 \cos\frac{G_x x_i}{d_x} + G_2 \sin\frac{G_x x_i}{d_x}\right) + \sigma_{m0} g_i / \sqrt{2}, \qquad i = 1, 2, 3, \cdots. \qquad (6)$$

Each of G_0, G_1, G_2, G_x (spatial frequency), and g_i (i = 1, 2, 3, …) in model (6) is an independent stochastic/random variable of mean zero and standard deviation one. The number of random variables for a group of N devices in model (6) is (N + 4). Model (6) leads to this spatial correlation,

$$c(x_i, x_j) = \frac{\sigma_{sys}^2}{\sigma^2} + \frac{\sigma_{acv}^2}{\sigma^2}\left\langle \cos\frac{G_x x_{ij}}{d_x} \right\rangle, \qquad i \neq j, \qquad (7)$$

which is translational invariant in the X direction and is a continuous function of separation $|x_{ij}|$. In a SPICE or TCAD simulation, the average operation, $\langle \cdots \rangle$, is accomplished through a Monte Carlo run. To make generated correlation function (7) identical to the given correlation function (5), we choose the distribution $f_x(G_x)$ of the random variable G_x being an integration over the product of the given spatial correlation and a cosine function:

$$f_x(G_x) = \frac{1}{\pi}\int_0^{+\infty} c_{acv,x}(u)\cos(G_x u)\, du. \qquad (8)$$

The distribution $f_x(G_x)$ is both symmetric and normalized.

The analytic solutions of several often discussed spatial correlation functions (Fig. 7) are given below. Each of the correlation function is always positive and decreases monotonically with increasing device separation.

(i) Gaussian decreasing type, $c_{acv,x}(u) = \exp(-\frac{1}{2}u^2)$: The distribution of random variable G_x happens to be also a Gaussian type, $f_x(G_x) = \exp(-\frac{1}{2}G_x^2)$. Note that all SPICE simulators provide the Gaussian type of random variables.

(ii) Exponential decreasing type, $c_{acv,x}(u) = \exp(-u)$: The distribution of random variable G_x is a Lorentz distribution with mean zero and a half width at half height being one, $f_x(G_x) = [\pi(1 + G_x^2)]^{-1}$.

(iii) Lorentz decreasing type, $c_{acv,x}(u) = (1 + \frac{1}{2}u^2)^{-1}$: The distribution of random variable G_x is an exponential distribution, $f_x(G_x) = \exp(-\sqrt{2}|G_x|)/\sqrt{2}$.

(iv) Linear decreasing type, $c_{acv,x}(u) = 1 - |u|, |u| \leq 1$; $c_{acv,x}(u) = 0, |u| \geq 1$. The distribution of random variable G_x is proportional to the square of a sinc function (Fig. 8), $f_x(G_x) = \sin^2(\frac{1}{2}G_x)/[2\pi(\frac{1}{2}G_x)^2]$.

In terms of adjacent mismatch σ_{m0}, distance-dependent mismatch σ_{acv}, and the normalized spatial correlation function $c_{acv,x}$, mismatch expression (1) becomes

$$\left\langle [P_i(x_i) - P_j(x_j)]^2 \right\rangle = \sigma_{m0}^2 + 2\sigma_{acv}^2[1 - c_{acv,x}(|x_{ij}|/d_x)]$$

Small-distance limit: For both (i) Gaussian and (iii) Lorentz decreasing types, mismatch increases quadratically with distance when the distance is small,

$$\left\langle [P_i(x_i) - P_j(x_j)]^2 \right\rangle = \sigma_{m0}^2 + \frac{\sigma_{acv}^2 x_{ij}^2}{d_x^2}, \quad \text{when } x_{ij}^2 << d_x^2 . \quad (9)$$

So Gaussian and Lorentz decreasing types of characterizations agree with Pelgrom's characterization at small distance [1]. For (ii) exponential and (iv) linear decreasing types, mismatch increases linearly with distance when the distance is small,

$$\left\langle [P_i(x_i) - P_j(x_j)]^2 \right\rangle = \sigma_{m0}^2 + \frac{2\sigma_{acv}^2 |x_{ij}|}{d_x}, \text{ when } |x_{ij}| << d_x. \quad (10)$$

Data shown in this paper are in this camp. Exponential and linear decreasing types of characterizations are different from Pelgrom's characterization at small distance.

Let the distance by which the normalized spatial correlation function $c_{acv,x}$ drops to 1% (50%) be u_{range} (u_{hwhm}). Then, the normalized correlation range $u_{\text{range}}/u_{\text{hwhm}}$ is (i. Gaussian) 2.58, (ii. exponential) 6.64, (iii. Lorentz) 10, and (iv. linear) 2.

Note that, when netlisting the ith device, none of other device's coordinates are needed. This is the compactness of our models for being able to model distance-dependent mismatch even without knowing other device's locations when the ith device is specified in a SPICE netlist or in a TCAD deck.

3.2 Two-dimensional Models

(i) *Solutions for separable 2D spatial correlations.*

When the ACV part $C_{acv}(u, v)$ of a two-dimensional (2D) spatial correlation function can be decomposed into the product of two one-dimensional (1D) spatial correlation functions,

$$C(\mathbf{x}_i, \mathbf{x}_j) = \frac{\sigma_{sys}^2}{\sigma^2} + \frac{\sigma_{acv}^2}{\sigma^2} c_{acv,x}\left(\frac{|x_{ij}|}{d_x}\right) c_{acv,y}\left(\frac{|y_{ij}|}{d_y}\right), \quad i \neq j, \quad (11)$$

our two-dimensional model for parameter P is

$$P(\mathbf{x}_i) = \mu + \sigma_{sys} G_0 + \frac{1}{\sqrt{2}} \sigma_{m0} g_i$$
$$+ \sigma_{acv}\left(G_1 \cos\frac{G_x x_i}{d_x} + G_2 \sin\frac{G_x x_i}{d_x}\right)\left(G_3 \cos\frac{G_y y_i}{d_y} + G_4 \sin\frac{G_y y_i}{d_y}\right),$$
$$i = 1, 2, 3, \ldots \quad (12)$$

In Eq. (12), each of G_0, g_i (i = 1, 2, 3, …), G_1, G_2, G_3, G_4, G_x, and G_y is an independent stochastic/random variable of mean zero and standard deviation one. The number of random variables for a group of N devices in model (12) is (N + 7). Similar to the above 1D model, the distribution $f_x(G_x)$ of the stochastic variable G_x is (8), and the distribution $f_y(G_y)$ of the random variable G_y is

$$f_y(G_y) = \frac{1}{\pi} \int_0^{+\infty} c_{acv,y}(v) \cos(G_y v)\, dv . \quad (13)$$

The distribution $f_y(G_y)$ is also symmetric and normalized.

A special isotropic correlation function. When a two-dimensional correlation function is of the elliptical Gaussian form,

$$C(\mathbf{x}_i, \mathbf{x}_j) = \frac{\sigma_{sys}^2}{\sigma^2} + \frac{\sigma_{acv}^2}{\sigma^2} \exp\left[-\frac{1}{2}\left(\frac{x_{ij}^2}{d_x^2} + \frac{y_{ij}^2}{d_y^2}\right)\right], \quad i \neq j, \quad (14)$$

each one-dimensional correlation function $c_{acv,x}(|x_{ij}|/d_x)$ [$c_{acv,y}(|y_{ij}|/d_y)$] is of the Gaussian form, and thus (14) can be represented by model (12) with the distribution of each random variable G_x and G_y being a Gaussian distribution. Notice that two-dimensional spatial correlation (14) is isotropic when the correlation range parameters d_x and d_y are equal, i.e., contours of constant correlation values form a set of concentric circles.

(ii) *Solutions for non-separable 2D spatial correlations.*

Our most general ACV model is

$$P(\mathbf{x}_i) = \mu + \sigma_{sys} G_0 + \frac{1}{\sqrt{2}} \sigma_{m0} g_i$$
$$+ \sigma_{acv}\left[G_1 \cos\left(\frac{G_x x_i}{d_x} + \frac{G_y y_i}{d_y}\right) + G_2 \sin\left(\frac{G_x x_i}{d_x} + \frac{G_y y_i}{d_y}\right)\right],$$
$$i = 1, 2, 3, \cdots . \quad (15)$$

Model (15) leads to this coupled 2D spatial correlation,

$$C(\mathbf{x}_i, \mathbf{x}_j) = c(x_{ij}, y_{ij}) = \frac{\sigma_{sys}^2}{\sigma^2} + \frac{\sigma_{acv}^2}{\sigma^2}\left\langle \cos\left(\frac{G_x x_{ij}}{d_x} + \frac{G_y y_{ij}}{d_y}\right)\right\rangle, \quad (16)$$

which is translational invariant in the X and/or the Y direction and is continuous. To make generated correlation function (16) identical to the given correlation function (4), we find that the joint probability distribution for both random variables G_x and G_y is

$$F(G_x, G_y) = \frac{1}{\pi^2} \int_0^{+\infty} du \int_0^{+\infty} dv\, C_{acv}(u, v) \cos(G_x u) \cos(G_y v), \quad (17)$$

which is symmetric in both G_x and G_y, and is also normalized. When $C_{acv}(u, v)$ is isotropic, (17) can be reduced to a one-dimensional integral involving the zeroth-order Bessel function, and the distribution $F(G_x, G_y)$ is also isotropic.

4 SUMMARY

We have shown that distance-dependent mismatch in semiconductor devices increases with distance but is not quadratic with distance in general, definitely not for large distance. For the first time, we have also presented a simple and complete solution of modeling any given 1D or 2D across-chip variation in simulations. The resulting spatial correlation is both translational invariant and continuous. The correlation range of the given spatial correlation can be much smaller than, be about, or be much larger than chip size. We use *only two* additional model instance parameters in our general compact solution. They are the physical location (x, y) of each device on a chip.

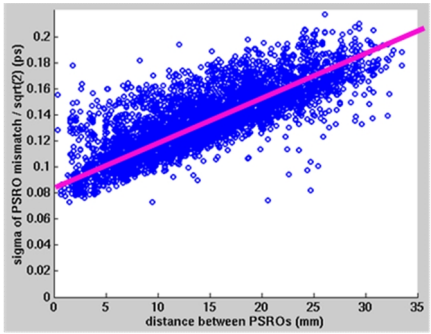

Fig. 1. Scatter plot of ring oscillator (RO) delay mismatch vs. RO separation. 87 ROs were put on a 22nm chip. There are 87x86/2 small circles in the figure. Pink line represents a characterized delay mismatch vs. distance relation from the data shown.

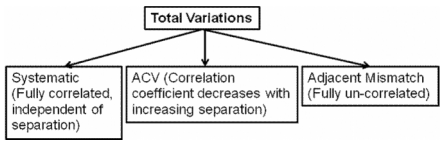

Fig. 2. Components of a parameter's total variation in terms of its correlation with the variation of the same parameter at other locations.

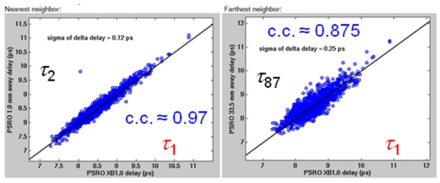

Fig. 3. Scatter plot between the delay of 22nm RO at a corner of the chip and that at its nearest neighbor (left). Scatter plot between the delay of RO at the corner and that at its farthest neighbor (right). Each plot shows measured data from 1450 chips on 135 wafers.

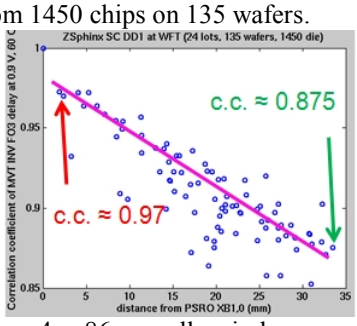

Fig. 4. 86 small circles are 86 correlation coefficients between the 22nm RO at the corner and ROs at 86 other locations. Pink line represents a characterized correlation coefficient vs. distance correlation.

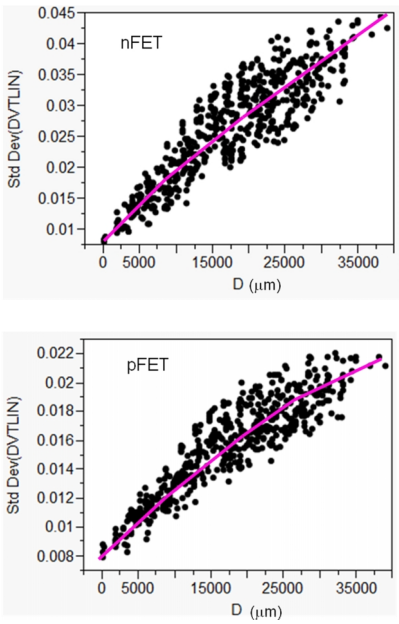

Fig. 5. Scatter plots of FET Vtlin mismatch data vs. device separation in 14 nm SOI FinFET technology. Pink curves are characterized mismatch vs. distance relations from the data shown.

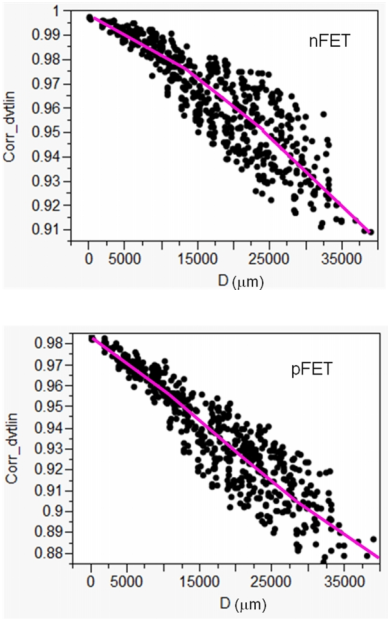

Fig. 6. Scatter plots of FET Vtlin correlation coefficient data vs. device separation in 14 nm SOI FinFET technology. Pink curves are characterized correlation coefficient vs. distance relations from the data shown.

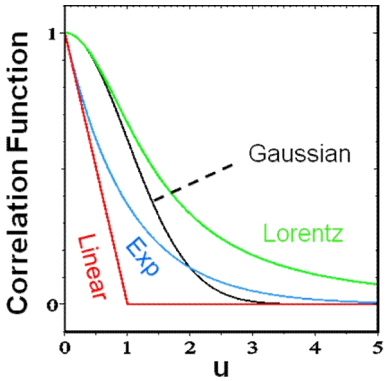

Fig. 7. Four kinds of often discussed spatial correlation functions.

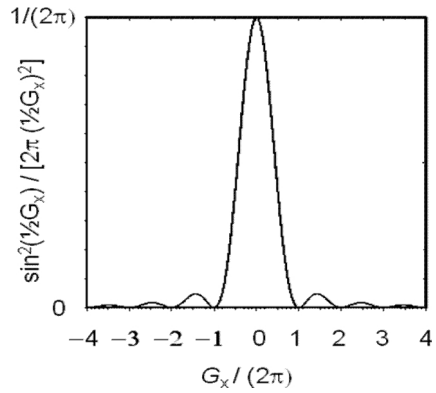

Fig. 8. Probability distribution of the spatial frequency G_x (a random variable) that leads to a linear decreasing spatial correlation function.

ACKNOWLEDGMENT

The authors thank former IBM colleagues for sharing SOI hardware data before joining Globalfoundries.

REFERENCES

[1] M. J. M. Pelgrom, *et al.*, *IEEE J. Solid-State Circuits*, p. 1433, 1989.

[2] T. B. Hook *et al.*, IEDM, p. 115, 2011.

[3] N. Lu *et al.*, IEDM, p. 852, 2014.

[4] A. Gattiker, *et al.*, in *Proceedings of the International Test Conference*, p. 1, 2006.

[5] R. Chen *et al.*, Asia and South Pacific Design Automation Conference, p. 310, 2008.

[6] S. Narasimha *et al.*, IEDM, p. 52, 2012.

[7] C.-H. Lin *et al.*, IEDM, 2014, p. 74, 2014.

[8] N. Lu, IEEE TED, Vol. 61, p. 342, 2014.